specific design (aspect ratio, etc.) and on the specific angle of trim, lift-to-drag ratios exceeding 4.

Full-scale unmanned drops and live jumps have demonstrated fast and reliable deployment (with and without reefing), excellent flight stability in free glide and under manned or automatic control. Fully flared landings with near zero landing velocity have been demonstrated through use of the para-foil's wide range of controlled trim angles ($-5° \leq \alpha \leq 90°$).

In applying the para-foil to various applications, it has been shown that 1) Controlled cargo delivery at drop speeds up to 130 KIAS can be accomplished with weights of up to 2000 lb. 2) Payload recoveries at dynamic pressures of 120 psf and at drop speeds of 350 fps have been demonstrated with 150 lb. 3) Tethered flights have been conducted to altitudes of over a mile for tracking, targetry and meteorological applications. 4) Numerous manned jumps and controlled landings have been accomplished. 5) Sustained manned-power flight and flare landings have been carried out.

Pare-foil designs for operation within the performance parameters discussed herein can be provided to satisfy current military and NASA requirements. Sufficient data are available for investigation of the para-foils capability to satisfy future military and NASA requirements.

References

[1] Nicolaides, J. D. and Knapp, C. F., "A Preliminary Study of the Aerodynamic and Flight Performance of the Para-Foil," July 8, 1965, Conference on Aerodynamic Deceleration, University of Minnesota.

[2] Nicolaides, J. D., "On the Discovery and Research of the Para-Foil," Nov. 1965, International Congress on Air Technology, Little Rock, Ark.

[3] Nathe, G. A., Knapp, C. F., and Nicolaides, J. D., "The Para-Foil and Targetry Applications," Feb. 8, 1966, Target Systems Planning Group, Hill Air Force Base, Ogden, Utah.

[4] Nathe, G. A., "An Analysis of the Para-Foil," April 21, 1966, Southwestern Student AIAA Competition, Graduate Div., Dallas, Texas.

[5] Nicolaides, J. D., Nathe, G. A., and Knapp, C. F., "A Summary of the Tests Conducted on the Para-Foil," June 8, 1966, Aerospace Engineering Dept., University of Notre Dame, Notre Dame, Ind.

[6] Nicolaides, J. D. and Knapp, C. F., "Para-Foil Design," UNDAS-866 JDN Rept., U.S. Air Force Flight Dynamics Lab., Wright-Patterson Air Force Base, Ohio.

[7] Knapp, C. F. and Barton, W. R., "Controlled Recovery of Payloads at Large Glide Distances, Using the Para-Foil," SC-R-67-1049, Nov. 1967, Sandia Laboratory, Albuquerque, N.Mex.

[8] Nicolaides, J. D., "Para-Foil Performance in Tethered, Gliding, and Towed Flight," Oct. 1969, Aero-Space Engineering Dept., University of Notre Dame, Notre Dame, Ind.

[9] Metres, S. R. et al., "Project Pin Point Review Report," Air Force Flight Dynamics Lab., Wright-Patterson Air Force Base, Ohio.

[10] Jehn, L. A., "Maximum Likelihood Solution to Theodolite Data," Rept. TR-68-15, March 1968, University of Dayton Research Institute, Dayton, Ohio.

[11] White, G. B. and Carranza, V., "Data Reduction-Computation Report Summary," JPTF Range Operations, Philco-Ford Corp., El Centro, Calif.

[12] Kane, M. T., Dicken, H. K., and Buehler, R. C., "A Homing Parachute System," SC-4537 (RR), Jan. 1961, Sandia Corp.

[13] Coonce, C. A., "Para-Foil Free-Flight Test Data," SCTM 66-2616, Dec. 1966, Sandia Laboratory.

[14] Nicolaides, J. D., "U.S. Army Jump Para-Foil," 1968, Aerospace Engineering Dept., University of Notre Dame, Notre Dame, Ind.

[15] Nicolaides, J. D. and Greco, J. R., "Para-Foil Wind Tunnel Tests," Nov. 1969, Aero-Space Engineering Dept., University of Notre Dame, Notre Dame, Ind.

[16] Roach, B., *A Wing and a Prayer*, Scholastic, University of Notre Dame, March 1965.

[17] Saar, J., *LIFE*, Sept. 1968.

SEPT.-OCT. 1970 J. AIRCRAFT VOL. 7, NO. 5

A Two-Dimensional, Mixed-Compression Inlet System Designed to Self-Restart at a Mach Number of 3.5

WARREN E. ANDERSON* AND NORMAN D. WONG†

NASA Ames Research Center, Moffett Field, Calif.

The methodology leading to the design of a Mach number 3.5 high-performance, two-dimensional, mixed-compression, inlet system with self-restart capability is reviewed. The principal feature of the design is a variable ramp system employing a flexible isentropic surface to provide efficient external compression ondesign and engine airflow matching with low spillage drag offdesign. An engine-face variable bypass system was also provided. Pertinent experimental results are presented for a range of Mach numbers from 1.55 to 3.5. Results show high over-all performance with moderate penalties associated with self-restart at Mach numbers of about 3.0 and above. Further bleed system optimization promises a means to eliminate these penalties and extend the self-restart capability to inlet systems of higher contraction ratios and thus potentially higher performance.

Nomenclature

A	= duct cross-sectional area
A_c	= inlet capture area, 196 in.^{2}
A_{LIP}/A_{THROAT}	= inlet contraction ratio
$(A_{LIP}/A_{THROAT})_{RESTART}$	= inlet restart contraction ratio (reference)
h	= height above surface, in.
M	= Mach number
M_1	= initial ramp Mach number
m_∞	= capture mass flow, $P_\infty V_\infty A_c$
m_{bl}/m_∞	= boundary-layer bleed mass-flow ratio
m_{by}/m_∞	= bypass mass-flow ratio
p_t	= total pressure
$\bar{p}_{t_2}$	= area-weighted average total pressure at engine-face station

Presented as Paper 69-447 at the AIAA 5th Propulsion Joint Specialist Conference, U.S. Air Force Academy, Colo., June 9–13, 1969; submitted September 25, 1969; revision received January 19, 1970.

* Research Scientist. Member AIAA.

† Research Scientist.

Δp_{t_2} = distortion index, $(p_{t_{2\max}} - p_{t_{2\min}})/\bar{p}_{t_2}$ at engine-face station
$\bar{p}_{t_2}/p_{t_\infty}$ = main duct total-pressure recovery ratio at engine-face station
V = velocity
ΔW_{a_c} = change in corrected airflow weight
α = angle of attack, deg
β = angle of yaw, deg
ρ = mass density
δ_1 = initial external compression angle, deg
δ_2 = isentropic external compression angle, deg

Subscripts

∞ = freestream
ζ = local
LIP = cowl lip leading edge
THROAT = inlet duct minimum cross-sectional area

Introduction

THE continuing challenge to improve the performance of supersonic aircraft places extreme demands on the art of advanced aircraft design. Success in meeting this challenge is closely allied to the advanced technology resulting from aeronautical research. Certainly a major factor in achieving higher performance is the aircraft air-breathing propulsion system of which the air-induction system is a major component. Recently, research on inlet aerodynamics has expanded as a result of the increased difficulty of providing airframe-engine compatibility over an ever increasing flight envelope. Also, advancing engine technology requires greater sophistication in the design of inlet systems.

Ames Research Center is conducting research programs to support the development of the inlet technology which is necessary for the design of high-performance supersonic and hypersonic aircraft. As a part of this effort, two large-scale, mixed-compression, two-dimensional inlet models have been built and tested to date. A sketch of the first model is shown in Fig. 1. The inlet design Mach number is 3.0 and some of the distinguishing features of the design are 1) the variable-ramp system for optimum inlet-engine matching, 2) relatively short subsonic diffusers utilizing vortex generators for low engine-face flow distortion, 3) porous boundary-layer bleed surfaces (shaded regions), and 4) a translatable, low-drag cowl.

Experimental tests with this model have been completed at Mach numbers from 0.6 to 3.2. Major conclusions from preliminary results[1-4] of these studies are as follows: 1) high compression efficiency can be obtained with a relatively short, potentially lightweight, low-drag system; 2) two-dimensional inlet systems offer the design flexibility to meet a wide range of engine placement and engine-airflow matching requirements with high over-all inlet efficiency; and 3) two-dimensional inlet designs for higher Mach numbers with a substantially greater amount of external compression to provide for a self-restart capability should be investigated experimentally.

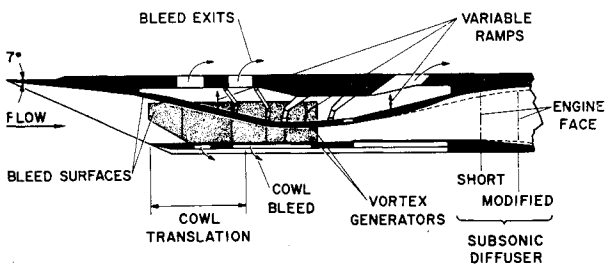

Fig. 1 Mach number 3.0 two-dimensional inlet.

These conclusions led to the design and test of a second inlet model with the design Mach number increased to 3.5. The inlet design criteria and merit of self-restart are discussed under model design. Wind-tunnel tests of this model have been completed at Mach numbers from 1.55 to 3.5 (Reynolds number/ft from 4.0–1.7 $\times$ 10^6, respectively). Model design and preliminary test results including comparisons between the two inlets are discussed on the following pages.

Model Design

A sketch of the Mach number 3.5 inlet design is shown in Fig. 2. Major design considerations as noted are 1) high external compression to provide a self-restart capability, high performance, and a short internal supersonic diffuser; 2) a variable ramp system employing a flexible, isentropic surface to provide efficient external compression ondesign and low spillage drag offdesign; 3) an internal supersonic diffuser and boundary-layer bleed system to provide a wide range of stable mass-flow ratio and to promote self-restart; and 4) a variable bypass system for studying the effect of flow bypass on engine-face flow distortion.

At design conditions the initial ramp oblique shock wave and the isentropic compression fan generated by the flexible ramp coalesce at a point slightly forward of the cowl lip leading edge. The theoretical internal shock-wave pattern as indicated in Fig. 2 consists of a single cowl-generated shock wave which is reflected internally. Supersonic diffuser contours were developed using the method of characteristics as programed in Ref. 4. Design of the subsonic diffuser was based on experience gained during tests with the first model and utilized vortex generators mounted on the ramp surface near the throat region.

The initial compression ramp angle δ_1 is fixed at 7° and the inlet capture height and width are both 14.0 in. The variable ramp mechanism is the same as for the first model with the exception of the addition of the external, flexible, isentropic surface. Boundary-layer bleed was accomplished with a series of perforated, replaceable plates on all four internal duct surfaces. The plates were perforated with $\frac{1}{16}$-in. drilled holes to a basic porosity of 12%. Various bleed patterns were obtained by filling holes to alter the bleed flow distribution. Three compartmented bleed plenums located above the ramp assembly are separated by hinged-plate dividers. Compartmentation of the bleed flow in this manner is provided to preclude recirculation because of longitudinal pressure gradients within the diffuser. The ramp bleed passed directly into the compartmented chambers and was exhausted through circular ducts located on top of the model. Side-wall bleed was ducted principally through passages within the sidewall structure into these chambers. A limited amount of forward sidewall bleed and all cowl bleed was exhausted directly overboard to the ambient airstream. All bleed exhaust areas were variable to provide mass-flow control.

Circular arc fillets provide the transition from the rectangular duct at the throat to a near circular engine-face station. The variable bypass system was sized to remove up to 30% of the capture mass flow at design conditions.

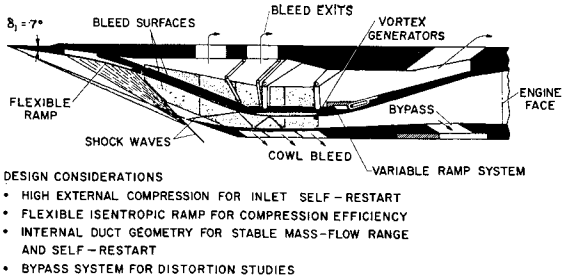

Fig. 2 Mach number 3.5 two-dimensional inlet.

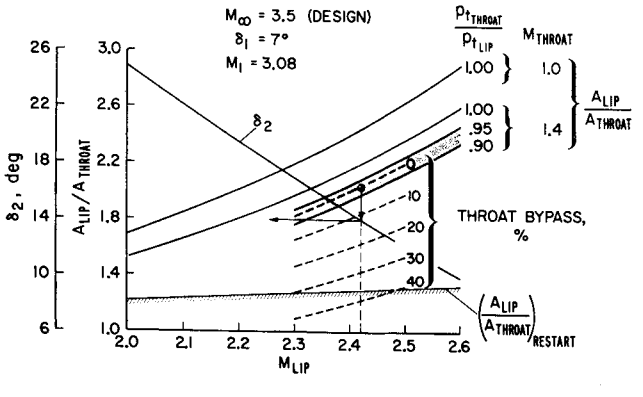

Fig. 3 Theoretical effect of lip Mach number on supersonic diffuser geometry.

Bypass mass flow was controlled by varying the bypass exit area with a remotely controlled slide plate. A fixed parabolic-shaped exit plug with translating sleeve is provided to control the main duct flow.

A self-restarting inlet system eliminates the need for a mechanical actuation of the inlet to return the propulsion system to normal operation after an excessive flight transient causes inlet unstart. A mixed-compression inlet system with self-restart capability can retain its inherently high internal performance and low drag benefits and achieve the relative simplicity of control of an external-compression inlet system. A detailed analysis of the self-restart cycle and the performance benefits which can accrue from such a system are reported in Ref. 3. Included in Ref. 3 are experimental results obtained from the first model (Fig. 1) which was modified to investigate self-restart performance. As expected, these data verify the importance of reduced lip station Mach numbers in the design of a self-restart inlet system. The relationship of lip Mach number to the conflicting geometric requirements between efficient supersonic diffusers and self-restart is shown in Fig. 3. One-dimensional continuity relationships and wedge-flow theory were used to compute the information shown by the curves. A single curve relates the external isentropic compression angle δ_2 to the lip Mach number for the present model (see flexible ramp in Fig. 2) based on the design Mach number of 3.5 and the initial 7° ramp. Knowledge of the total external flow turning angle measured from the horizontal reference plane ($\delta_1 + \delta_2$) is necessary to determine the internal cowl angle required for the desired internal shock-wave pattern. Although increasing δ_2 decreases the cowl lip Mach number, it also requires an increase in internal and external cowl angle which results in higher cowl drag.

The allowable inviscid contraction ratio values for self-restart are shown by the lower boundary in Fig. 3.‡ In contrast, the significantly larger values required for efficient supersonic diffusers are indicated by the family of curves at the top. The inlet contraction ratio requirement is shown to be substantially reduced from the maximum by designing for an upper-limit throat Mach number of 1.4, and by accepting a throat total-pressure recovery as indicated by the shaded region. Even with this approach, a large percentage of the inlet lip station mass flow must be permitted to bypass the throat, if self-restart performance is to be achieved. Throat bypass mass-flow ratio curves superimposed on Fig. 3 indicate that bypass mass-flow ratios of 30–40% are required for self-restart at lip Mach numbers from 2.3 to 2.5. Lip Mach numbers of this magnitude are required to permit the low external turning angles which are necessary for low cowl drag. However, the large throat bypass mass flow required for self-restart can represent a significant problem.

‡ Calculation assumes an external normal shock wave occurring at the lip Mach number.

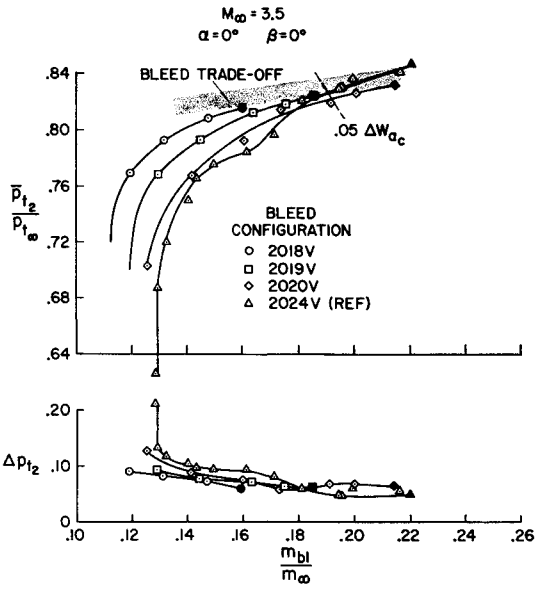

Fig. 4 Maximum performance showing bleed configuration effects.

Since throat bypass for self-restart need only occur during the actual restart process, attention is naturally focused on the steady-state boundary-layer bleed system and the capacity of such a system to provide the needed bypass. On the basis of predictions of required steady-state boundary-layer bleed mass flow at design conditions and of the capability of the resulting bleed system to bypass mass flow during an unstarted condition, the design inlet lip Mach number was set as 2.42 for an inlet-throat-to-lip total-pressure recovery of 0.93 and a throat Mach number of 1.4. (In establishing these design values consideration was also given to the criterion[3] which suggests that controlled boundary-layer separation forward of the lip acts to reduce the internal bypass requirement for restart.) As indicated on Fig. 3, the external isentropic compression angle required is 14° for a total external turning angle of 21°. A processing of these basic geometric values via the computer program resulted in a value for the internal cowl angle of 11°. On the basis of structural requirements the external cowl angle was in turn established at 18°. Reasonably low values of cowl pressure drag were calculated for angles of this level.

Results and Discussion

Results of wind-tunnel tests at the inlet design Mach number of 3.5 are shown in Fig. 4. Total-pressure recovery and distortion index obtained from engine-face rake measurements are plotted against boundary-layer bleed mass-flow ratio for four bleed configurations attaining the best recovery vs bleed tradeoff performance. The letter V following the bleed configuration identification number indicates the use of vortex generators. None of the configurations were self-restarting at the optimum throat heights (contraction ratios) for which data are presented; consequently, the curves represent the maximum attained performance of the inlet under conditions where it cannot self-restart. The solid symbols indicate the peak recovery conditions prior to inlet unstart. Configuration 2024V provided the highest peak recovery value, 0.846 at a bleed mass-flow ratio of 0.22. At this peak value, a low distortion index of 0.05 was measured. A supercritical bleed mass-flow ratio of 0.13 was measured for this configuration providing a relatively wide range of stable operation (approximately 0.09) with low distortion. Inlet operation with a control tolerance of 5% corrected weight flow is indicated to occur at a recovery of 0.826 and a bleed mass-flow ratio of 0.19. The other bleed configurations utilized successively

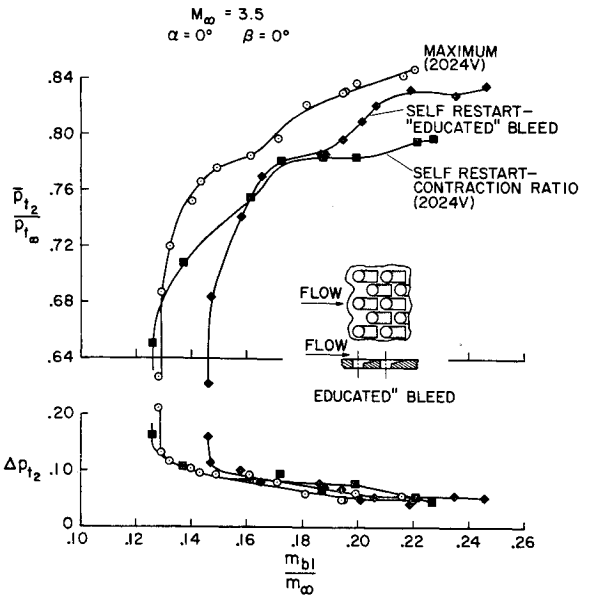

Fig. 5 Self-restart performance showing penalty for self-restart.

less boundary-layer bleed in the throat region of the duct which provided proportionately lower peak recovery and a smaller stable range but equivalent distortion. On the basis of the peak recovery values, a shaded band is indicated which is believed to represent an attainable tradeoff of bleed mass-flow ratio for reduced peak total-pressure recovery.

Further test results obtained at $M_\infty = 3.5$ are presented in Fig. 5. Two self-restart performance curves are compared to the maximum performance curve obtained with the optimum bleed configuration (2024V) which is repeated from the previous figure. Operation of this bleed configuration at the maximum self-restart contraction ratio (lower curve) results in a 0.05 reduction in peak recovery with little change in bleed mass flow or distortion index. A 10% decrease in contraction ratio was necessary to allow self-restart and throat region measurements show the throat Mach number increased from about 1.35 to 1.50. The additional terminal shock losses which are associated with this higher throat Mach number account for the lower recovery level. The curve labeled "educated" bleed in Fig. 5 represents performance with the bleed system modified to allow self-restart without decreasing contraction ratio. Bleed porosity was about doubled on the ramp surface in the region of the cowl lip station to provide the higher throat bypass flow required to self-restart. In an effort to preclude increases in bleed mass flow during normal operation, a form of "educated" bleed hole geometry was utilized in the regions where porosity was increased. A similar technique[5] theoretically reduced the hole flow coefficient for supersonic approach velocities to half that for the normal drilled hole. Thus, the "educated" holes would compensate for the additional bleed porosity. At subsonic approach conditions such as occur during unstart, the flow coefficient remains that of a normal hole and the additional bypass is realized. As shown by the sketch in Fig. 5, each hole was modified with an aft-ramp cutout which diverts some of the air that would ordinarily be turned into the hole back to the supersonic stream. This feature was only marginally successful as indicated by the 0.015 increase in supercritical bleed mass-flow ratio measured for the self-restart "educated" bleed configuration. However, the system did allow self-restart for a penalty in peak recovery of only 0.015. Distortion performance is unchanged from that of the maximum performance case. The previous comparison suggests that a better bleed configuration, particularly the application of a more successful "educated" bleed geometry, would provide a self-restart capability without reducing the maximum performance potential of the inlet system at a Mach number of 3.5.

Figure 6 summarizes peak recovery performance for both two-dimensional inlet models. Total-pressure recovery ratio, boundary-layer bleed mass-flow ratio and distortion index are plotted for a range of Mach numbers from 1.55 to 3.5. At Mach numbers of 1.55 and below both inlets operate as external compression systems. The results show generally that the performance trends established by the $M_\infty = 3.0$ design (dashed line) can be maintained up to a design Mach number of 3.5. The shaded region indicates the reduction in recovery when contraction ratio is limited to permit self-restart. As shown, recovery is not compromised by contraction ratios for self-restart at Mach numbers below 2.5. Also, for such self-restart systems, bleed mass-flow and distortion characteristics are equal to those for the maximum performance configuration over the full range of Mach numbers. A large bleed penalty results from using "educated" bleed self-restart at the Mach numbers tested (2.5–3.5). However, recovery also exceeds that for the maximum performance configuration by a substantial margin for most of this Mach number range. Undoubtedly, for equal recoveries the bleed penalty for self-restart could be substantially reduced from that shown for Mach numbers of 2.5 and 3.0.§ In summary, the results indicate that self-restart is potentially compatible with maximum performance over the full range of mixed compression operation. Further optimization of the bleed system with "educated" bleed geometry, is believed to offer a means of extending self-restart capability to inlet systems of higher contraction ratios and thus of potentially higher performance.

Additional test results for the maximum performance reference configuration are presented in Figs. 7–10. In Fig. 7, the

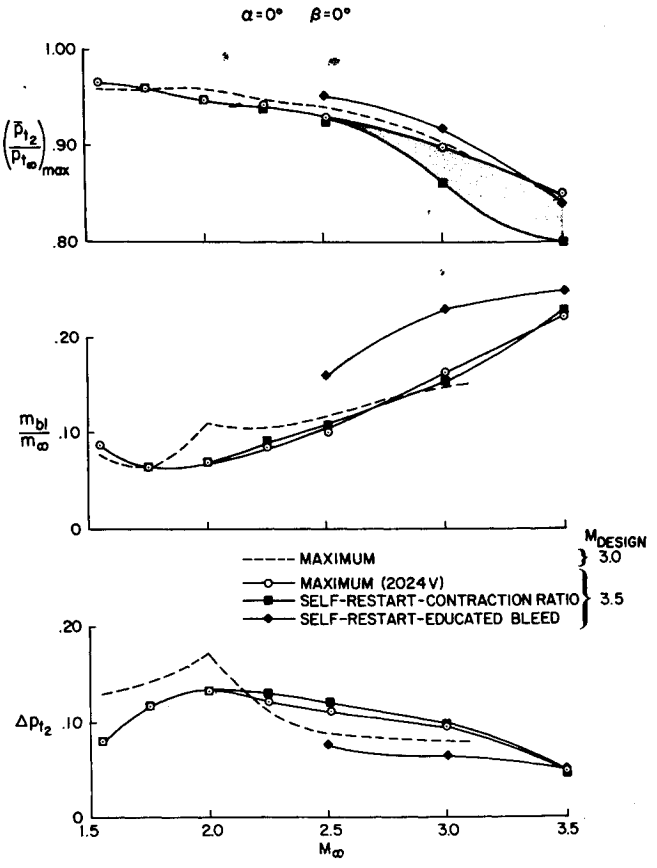

Fig. 6 Summary of maximum recovery performance.

§ Increasing throat height would reduce recovery and allow bleed to be reduced.

effects of steady-state angle of attack and angle of yaw on peak recovery performance are shown for representative Mach numbers from 3.5 to 1.55. A decrease in Mach number from 3.5 to 3.0 significantly reduces the adverse effect of angle of attack on maximum recovery above about $\alpha = 1°$. Recovery is reduced at $M_\infty = 3.5$ from 0.846 to 0.765 (0.08) for an increase in angle of attack from 0° to 6°. A similar change in angle of attack at a Mach number of 3.0 results in a loss in recovery of only 0.025. At lower Mach numbers the loss due to an equivalent change varies from 0.01 to 0.03. Inlet sensitivity to angle of yaw is substantially greater than that for angle of attack at Mach numbers of 2.5 and above. Boundary-layer-bleed characteristics were omitted from Fig. 7 since bleed mass flow was found to be relatively insensitive to flow angle variations. Distortion index is also insensitive to flow angle at Mach numbers other than 2.5 and 3.5. At $M_\infty = 3.5$ the increase in distortion is logically associated with the decrease in recovery mentioned previously; however, reasons for the distortion variations at $M_\infty = 2.5$ are not clearly understood. An important characteristic of two-dimensional inlets with horizontal ramps is the increase in supercritical capture mass-flow ratio with increasing angle of attack. As a result, moderate positive angle-of-attack transients will cause the inlet to unstart if sufficient operating tolerance is not provided. Tolerance to such transients is provided by increasing the throat Mach number and as such is compatible with the self-restart inlet design concept. The angles of attack at which the present inlet unstarts when the throat height is set for operation at $\alpha = 0°$ are identified in Fig. 7 ($M_\infty = 2.50$ and 3.50). A tolerance to transient angle-of-attack variations up to about 3° is indicated which is substantially more than the tolerance usually available to inlets of this type. Tolerance to negative angle of attack and angle of yaw was of the same magnitude. Therefore, inlet-control system response characteristics which might otherwise be required to prevent unstarts in the presence of gusts, passing aircraft, etc., can be reduced.

An interesting aspect of the experimental effort was the documentation of internal boundary-layer characteristics on the ramp, cowl, and side-wall surfaces. Local total-pressure recovery ratio and Mach number profiles are presented in Fig. 8 for supersonic diffuser and throat region loca-

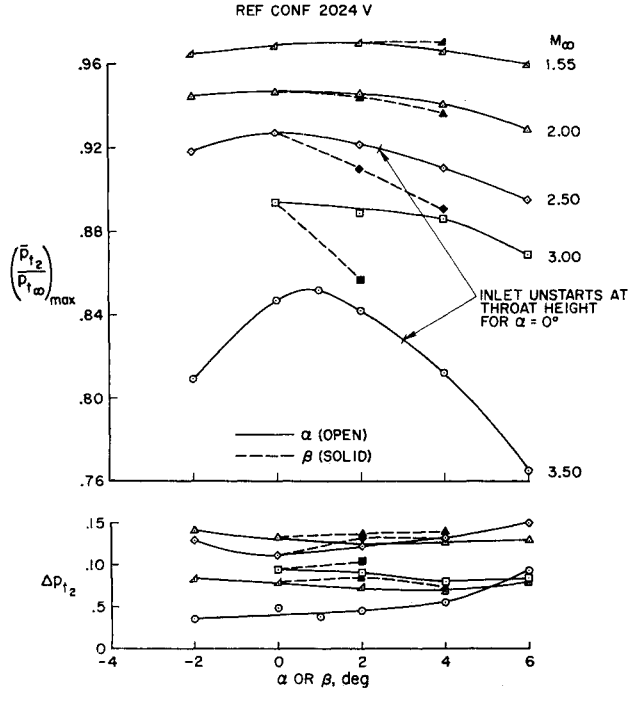

Fig. 7 Effects of α and β on maximum recovery performance.

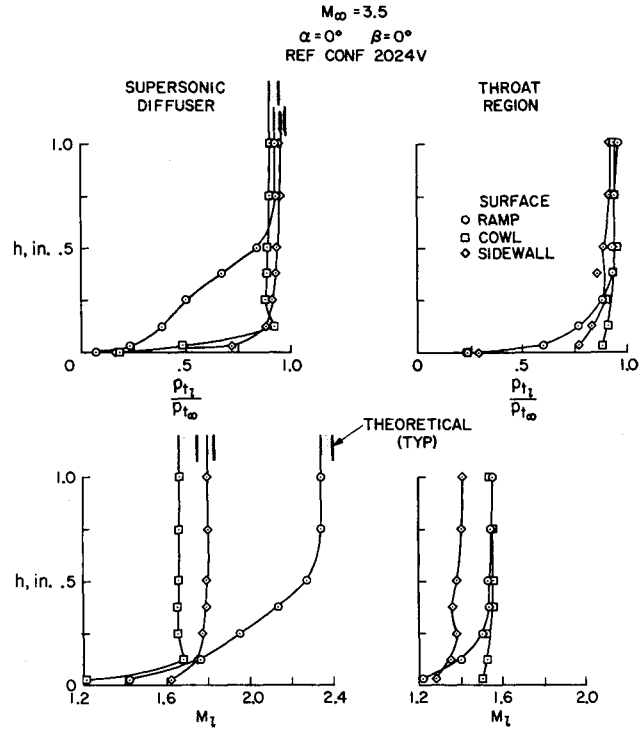

Fig. 8 Diffuser boundary-layer profile characteristics.

tions at the design Mach number. A super-critical bleed mass-flow condition (0.13) is considered with the terminal-shock wave located downstream of the throat rakes. The profiles span the boundary layer and show generally that both Mach number and pressure recovery agreed reasonably well with theoretical predictions. The ramp supersonic diffuser rake was located forward of the cowl-generated oblique shock wave and therefore measured the inlet lip station flow conditions. Boundary-layer bleed was not applied in any significant amount forward of this rake; therefore, large viscous losses are indicated. In contrast, the cowl and side-wall rakes were positioned downstream of the cowl shock-wave on surfaces having the benefit of boundary-layer control. Losses indicated by these rakes were minimal. Core flow recovery and Mach number as measured in the supersonic diffuser show some disagreement with theoretical predictions (shaded band). Both recovery and Mach number in a supersonic stream are sensitive to static pressure and the lack of accurate static pressure profile measurements in the core region could easily account for the indicated discrepancies. The ramp supersonic diffuser rake measured an inlet lip station Mach number of 2.34 compared to a theoretical value of 2.40. The throat rakes were located somewhat downstream of the geometric throat and therefore would be expected to register Mach numbers outside the boundary layer somewhat higher than the throat values because of supersonic expansion. The Mach numbers shown for the ramp and cowl are consistent with the predicted rake station values, implying the actual throat Mach number was approximately equal to the design value of 1.4. Side-wall rake measurements indicate a Mach number of 1.4 which suggests local expansion was not present between the throat and the side-wall rake station. Surface static pressures also show negligible expansion in this region.

Bypass system operation showed negligible effect on engine-face pressure recovery as shown in Fig. 9. Although the amount of bypass mass flow was somewhat restricted by the limited capacity of the system, up to 25% of the capture mass flow was bypassed in a localized region on the cowl side of the subsonic diffuser. Localizing the bypass flow area in this manner might be expected to cause distortion effects (flow

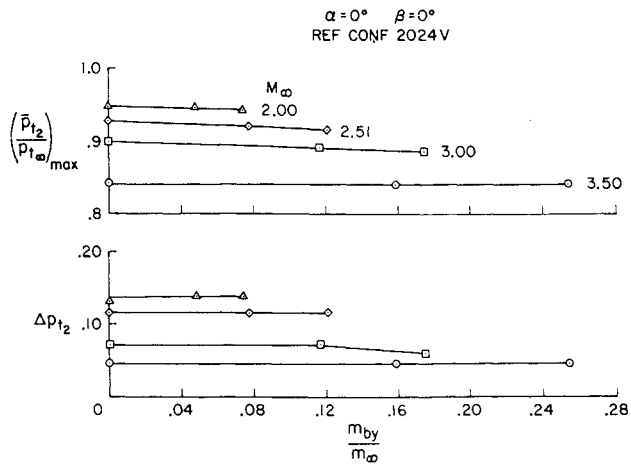

Fig. 9 Bypass mass-flow ratio effects on maximum recovery performance.

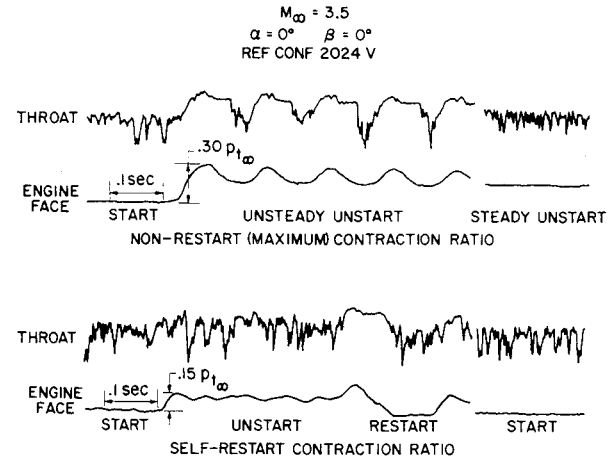

Fig. 10 Diffuser static-pressure unsteadiness characteristics.

asymmetry). But the data indicate that only at $M_\infty = 3.0$ was the distortion index affected to any noticeable degree.

Static-pressure unsteadiness during unstart is shown in Fig. 10 for the design Mach number of 3.5. Static pressure transducers were located at both throat and engine-face duct locations and trace recordings are shown for both maximum and self-restart contraction ratios. In each case, the inlet was brought to the minimum stable operating condition and then unstarted by closing the main mass-flow control plug area. Upon inlet unstart the plug area was opened to simulate increased engine airflow demand. Inlet restart occurs only for the self-restart contraction ratio although the maximum contraction ratio case progressed from an unsteady (buzz) to a steady mode of unstart. It appears that a self-restarting system has the characteristic of softening the degree of unsteadiness at the engine face which is associated with inlet unstart. For the nonrestart inlet the initial unstart transient reduces the duct static pressure by about 37% ($p_2/p_{t_\infty} \simeq 0.8$) followed by duct buzz at about 10 cycles/sec. The self-restart configuration unstarts with a transient of about half that amplitude and continues with a mild, rather random unsteadiness until restart occurs. Contraction ratios for the two cases differ by only 10% since the inlet was originally designed to self-restart at the maximum contraction ratio condition. Inlets designed without consideration for self-restart would operate at higher maximum contraction ratios and the unsteadiness during unstart would be more severe than that shown.

Concluding Remarks

It has been shown that a self-restart design is compatible with high performance for a two-dimensional mixed-compression inlet system designed for a Mach number of 3.5. The inherent nature of such a design provides good angle-of-attack performance with substantial tolerance to transient angle-of-attack variations. Also, the static-pressure unsteadiness associated with inlet unstart is significantly less for a self-restarting system than for higher contraction ratio nonrestarting types.

References

[1] Sorensen, N. E. et al., "Performance Summary of a Two-Dimensional and an Axisymmetric Supersonic Inlet System," TM X-1302, 1966, NASA.

[2] Anderson, W. E., Peterson, M. W., and Sorensen, N. E., *An Evaluation of Transonic Spillage Drag Based on Test Results from Large-Scale Inlet Models*, SP-124, NASA, 1966.

[3] Young, L. C., "Test Results of a Self-Starting Supersonic Mixed Compression Inlet," AIAA Paper 65-409, Colorado Springs, Colo., 1965.

[4] Anderson, W. E. and Wong, N. D. "Experimental Investigation of a Large Scale, Two-Dimensional, Mixed Compression Inlet System—Performance at Design Conditions, $M_\infty = 3.0$," TM X-2016, 1970, NASA.

[5] Sorensen, V. L., "Computing Program for Calculating Flow Fields in Supersonic Inlets," TN D-2897, 1965, NASA.

[6] McLafferty, G., "A Study of Perforation Configurations for Supersonic Diffusers," Rept. R-53372-7, Dec. 1950, Research Dept., United Aircraft Corp.